Advanced Sensors and Instrumentation

Issue 22 • March 2025

ASI Program Update

Pattrick Calderoni
Idaho National Laboratory
ASI National Technical Director

Welcome to the 22nd edition of the ASI program newsletter, dedicated to showcasing innovative research in the area of nuclear instrumentation and the people that make it happen. This issue is focused on the use of innovative sensors and measurement methods for the operation of advanced reactors. More specifically, we highlight research activities that fall in the two main research areas in which the ASI program has engaged: reactor power monitoring and structural health monitoring for advanced-reactor core components. Both areas leverage ASI expertise on instrumenting irradiation experiments in material test reactors, emphasizing the synergy that exists among the different technical areas of the ASI program.

Previous newsletters, including the most recent one on embedded sensors, showcased sensor technology advancements that warrant consideration regarding their use in advanced reactor cores. Sensors have been tested at temperatures compatible with normal and off-normal operation of proposed design concepts, and have been irradiated to gamma/neutron fluence levels that build confidence in their reliability over periods compatible with operational lifetimes or core-component maintenance strategies. The ASI program is now moving toward optimization of sensor functions and investigation into their integration with control systems and plant operation and maintenance.

One key element in the transition from "how" to reliably measure a specific parameter (e.g., neutron flux) to "what" to use the measurement for (e.g., monitoring

Continued on next page

In this issue...

For more program information, including recent publications, please visit www.asi.inl.gov

U.S. DEPARTMENT of ENERGY | Office of Nuclear Energy

Continued from previous page

reactor power) is sensor placement. Irradiation experiments have shown instrumentation to be an inherent part of design iterations, and that sensors cannot be added as an afterthought, even if off-the-shelf solutions exist. Optimizing the number and location of instruments is essential not only to avoid redundance and minimize costs, but also to enable the measurement system to satisfy the requirements for which it was designed.

This newsletter showcases research activities in which analysis of sensor locations is key to enabling the sensors' intended function. Such analysis is performed using tools and following approaches ranging from physics-informed to data-driven models, but all of which contribute to understanding the role of advanced sensors and instrumentation in designing and operating advanced reactors.

Sensor Placement for Core Power Distribution Reconstruction in a Nuclear Reactor

Haoyu Wang
Argonne National Laboratory

Roberto Ponciroli
Argonne National Laboratory

Richard B. Vilim
Argonne National Laboratory

Vasileios Theos
Purdue University

Stylianos Chatzidakis
Purdue University





Over the life of a reactor core, power distribution undergoes perturbations caused by fuel burnup, variations in coolant conditions, neutron poison build-up and control rod maneuvering. Traditional reconstruction techniques rely on a large number of in-core sensors placed at various locations. While this approach is commonly used in Light Water Reactors [1], it is not suitable for Advanced Reactors and Microreactors. In Advanced Reactors, harsh operating conditions render most of the commercially available in-core detectors impractical [2], while in Microreactors, the tight lattice pitch designed for maximum power density significantly restricts sensor placement.

A collaborative research team from Argonne National Laboratory (H. Wang, R. Ponciroli, R.B. Vilim) and Purdue University (V. Theos, S. Chatzidakis) has been developing a highly adaptable method for accurately reconstructing the core power distribution in a nuclear reactor since Fiscal Year (FY) 2024, by integrating physics-informed machine learning, high-fidelity modeling, and primarily ex-core real-time measurements, thus minimizing reliance on in-core detectors.

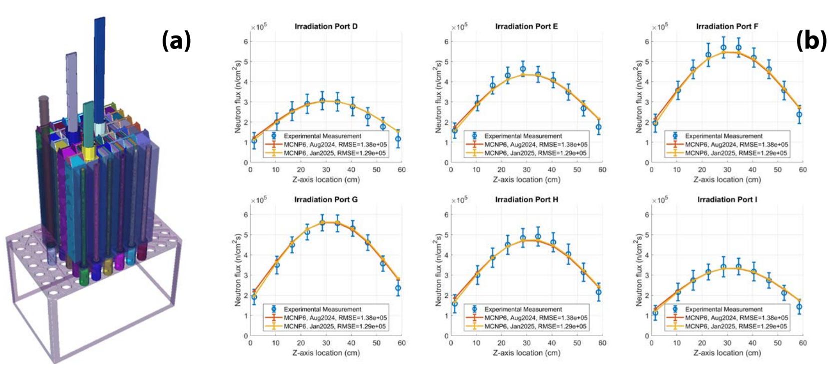

Figure 1. (a) Geometry and (b) Preliminary Experimental Validation of PUR-1 Neutronics Model

In FY2024 and FY2025, the team accomplished the theoretical formulation of the core power reconstruction method, and performed the preliminary experimental validation of the high-fidelity neutronics model of Purdue University Reactor Number One (PUR-1, Figure 1). Currently, the team is implementing and improving the core power reconstruction algorithm based on Convolutional

Continued on next page

Continued from previous page

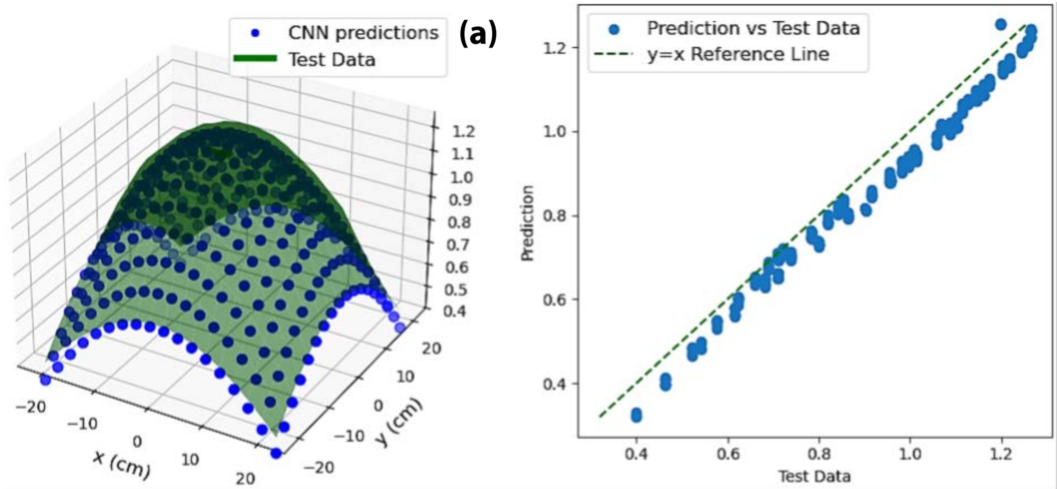

Figure 2. (a) Visualization of the CNN-predicted flux field (blue dots) overlaid on the test data (green surface) at 308 in-core locations. (b) Scatter plot comparing predicted and test values.

Neural Network (CNN), with promising results achieved on a simple test case (Figure 2)[3]. In addition, the team is also investigating the method to optimize control rod maneuvering using the information leant when training the CNN. In the upcoming FY2026, the team expects to finalize the sensor placement optimization and to perform a test on reconstructing the core power of PUR-1.

The major impact of this method is to support control optimization in nuclear reactors, enhancing economic performance based on user-defined metrics related to core power distribution [4]. Benefits could include better fuel utilization and outage scheduling [1], higher energy production through thermal margin recovery, and enhanced efficiency in radioisotope production.

References

[1] A. Birri, K.C. Goetz, D.C. Sweeney, N.D. Bull Ezell, "Towards Realistic and High Fidelity Models for Nuclear Reactor Power Synthesis Simulation with Self-Powered Neutron Detectors," ORNL/TM-2023/3009, Oak Ridge National Laboratory, Oak Ridge, TN (2023).

[2] K. Tsai, "Development of Temperature Compensation Tools for SPNDs Operating in High Temperature Environments," INL/RPT-22-69883 Revision 0, Idaho National Laboratory, Idaho Falls, ID (2022).

[3] H. Wang, R. Ponciroli, R.B. Vilim, V. Theos, S. Chatzidakis, "A Data-Driven Approach to Core Power Distribution Reconstruction in a Nuclear Reactor", manuscript submitted to Nuclear Plant Instrumentation and Control & Human-Machine Interface Technology (NPIC&HMIT 2025), June 15-18, 2025, Chicago, IL.

[4] R. Ponciroli and R.B. Vilim, "Strategy to Develop a Control Scheme for Core Thermal Performance Optimization," ANL/NSE-24/23, Argonne National Laboratory, Lemont, IL (2024).

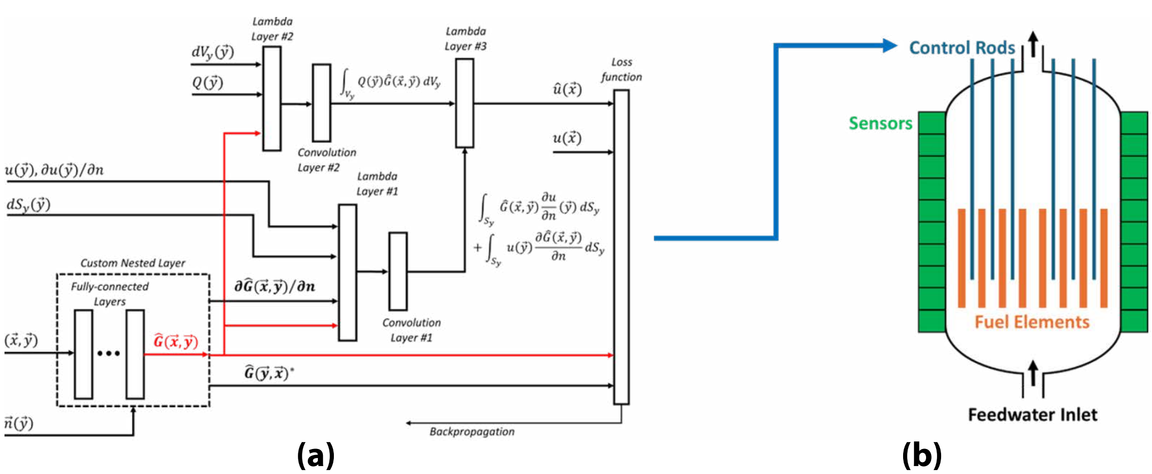

Figure 3. (a) Configuration of the proposed CNN during the training stage. (b) The trained Green's function will be used to optimize the control rod maneuvering during the testing stage.

Assessing Effects of Sensor Uncertainty, Degradation, Fuel Burn-up, and Anomalous Conditions on Core Power Synthesis

Anthony Birri
Oak Ridge National Laboratory

K. C. Goetz
Oak Ridge National Laboratory

Jianwei Hu
Oak Ridge National Laboratory

N. Dianne Bull Ezell
Oak Ridge National Laboratory

Introduction

Online monitoring of nuclear reactors involves the synthesis of the power distribution using a combination of in-core and ex-core radiation sensors. The accurate and timely synthesis of the core power distribution allow for operators to ensure that anomalous conditions, which could arise from accident scenarios (loss-of-coolant, cladding rupture, reactivity-initiated accident) or typical reactor operations (xenon oscillations, control rod movements), do not result in localized power peaking to violate safety limits. Power synthesis methods have been implemented for decades in commercial reactors to perform these necessary operations [1], but what is unclear is the extent to which these methods are optimized in terms of sensor placement, error reduction, and computational demand. To address this, there has been ongoing work [2-5] at Oak Ridge National Laboratory, funded by the Department of Energy, Office of Nuclear Energy, to conduct studies of power synthesis, in which certain variables are parameterized, such as sensor locations, sensor uncertainties, convergence criteria, and reactor conditions, in order to understand the impacts of these variables on the ability to accurately synthesize the power distribution, and resolve potential discrepancies which may occur for physics-based reasons.

Methods

The studies that have been conducted to simulate power synthesis have utilized the point-based iterative (PBI) method [2], which is fundamentally a response function-based method that resembles commercially patented methods. The method can be simply understood as a 5-step process: 1) use a neutronics model to estimate the power distribution, 2) calculate signal contributions (i.e. response functions) from individual chunks of fuel to the in-core and ex-core sensors using a nuclear transport code, 3) collect (or simulate) measured responses to potentially anomalous reactor conditions, 4) update the response-function equations in an iterative scheme, and 5) minimize the residual to finalize the solution. This fiscal year, a combination of neutronics and transport codes are being leveraged to perform steps 1 and 2, which are PARCS and MCNP6, respectively. The effect of assessing isotopic inventory changes in self-powered neutron detectors (SPNDs) as a function of reactor operation time is an ongoing effort; SCALE/ORIGEN is used for the inventory calculations, and Geant4 is used to model electron transport in the SPNDs, which is used to calculate electric current in the sensors.

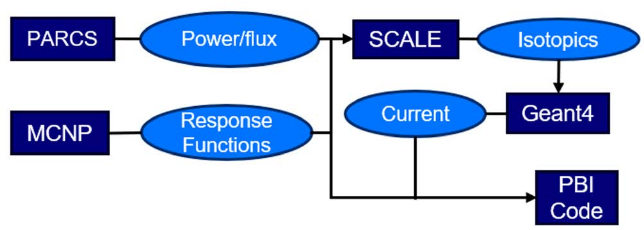

Figure 4. A flowchart which shows the data transfer between various codes to simulate power synthesis. Boxes indicate codes, while circles indicate data packets.

A flowcart is shown in Fig. 4, which shows the data transfer process between these codes, and how they ultimately feed a custom PBI code maintained at ORNL. The reactor design that is being used to conduct this study this fiscal year is a pressurized water reactor design, which is similar to an AP1000, which has been previously used to assess the impacts of using LEU+ fuel (i.e., with fuel enrichment higher than 5%); the beginning-of-cycle (BOC) power distribution for this core is shown in Fig. 5 [6].

Example Calculation

A preliminary calculation has been performed to illustrate the effect of the fuel burn-up on the accuracy of the synthesis. In this case, the SPNDs are assumed to have minimal current reduction (which is a simplifying assumption which is being further investigated). The initial estimate of the power distribution is based on the BOC conditions, while the sensors are responding to the core history after a total burn-up of 823 MWd/MTU; this allows for the isolation of this burnup effect on the

Continued on next page

Continued from previous page

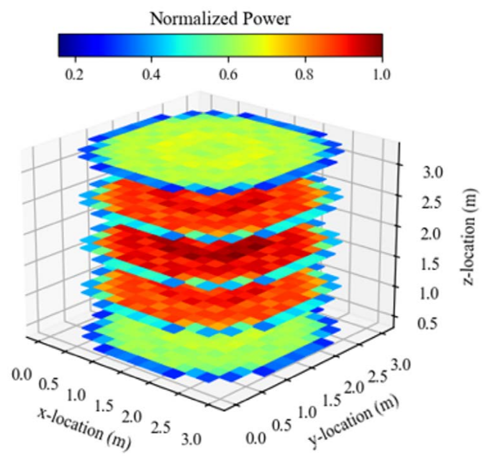

Figure 5. 3D power distributions calculated by PARCS in a representative PWR core [6]

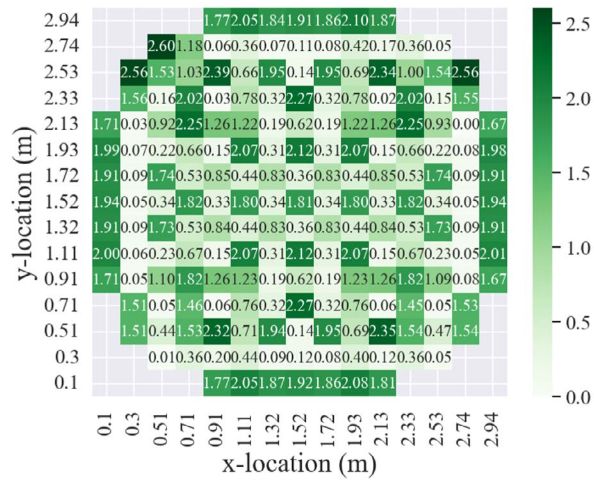

Figure 6. Percent error in the synthesized power distribution of a representative PWR core where the sensors are responding to fuel burnup of 823 MWD/MTU

synthesis accuracy. The resultant error in the radial power distribution is shown in Fig. 6. This example is intended to illustrate how one particular variable (burn-up) can affect the power distribution accuracy if it is not accounted for in a priori assumptions; the power of this framework and the flexibility of the PBI code is that several other variables can be readily parameterized, which allows for a simulation tool that can provide go/no-go assessments of different sensor configurations, optimization studies to identify error reduction strategies, and trade-off realizations related to calculation runtime versus accuracy.

References

[1] Boyd, William A., and R. Wade Miller. "The BEACON on-line core monitoring system: functional upgrades and applications." In Proc. Specialists' Meeting "In-core instrumentation and core assessment. 1996.

[2] Birri, Anthony, Daniel C. Sweeney, and N. Dianne Bull Ezell. Progress in Nuclear Energy 153 (2022): 104437.

[3] Birri, Anthony, K. Callie Goetz, Daniel C. Sweeney, and Nora Ezell. Report No. ORNL/TM-2023/3009. Oak Ridge National Laboratory (ORNL), 2023.

[4] Birri, Anthony, Jonathan T. Gates, Daniel C. Sweeney, Kathleen C. Goetz, and N. Dianne Bull Ezell. Progress in Nuclear Energy 172 (2024): 105200.

[5] Birri, Anthony, K. Callie Goetz, Daniel C. Sweeney, and N. Dianne Bull Ezell. Report No. ORNL/TM-2024/3567. Oak Ridge National Laboratory (ORNL), 2024.

[6] Hu, Jianwei, Ugur Mertyurek, and William A. Wieselquist. Report No. ORNL/TM-2022/1831. Oak Ridge National Laboratory (ORNL), 2022.

Reactor Dosimetry Program Support for ASI

Tommy Holschuh
Idaho National Laboratory

Teancum Quist
Idaho National Laboratory

David Chichester
Idaho National Laboratory

During irradiation experiments, an important variable to measure is the energy spectrum of the neutrons in the irradiation environment, or more precisely, the neutron energy spectrum that irradiated a particular experiment position or capsule. Within a given nuclear reactor, the distribution of neutron energies can drastically change based on the relative position of the neutron sources (fuel), poisons (control rods), or structural materials (e.g., steel and aluminum). Additionally, intentional flux shaping materials, such as cadmium or gadolinium, can alter the energy distribution. Attenuation through experiment capsules can also alter the energy profile.

Reactor dosimetry incorporates materials, typically in the form of thin-diameter wires (~0.5 mm) or thin foils, into an experiment capsule or irradiation cavity to interact with the neutron fluence. Each isotope has a unique neutron cross section as a function of neutron energy, and new isotopes are produced in the foils or wires when neutrons are absorbed (thermal neutrons) or interact in other ways (fast neutrons). The materials for the foils or wires are chosen such that the created isotopes have measurable gamma-ray emissions, as well as half-lives sufficiently long to reflect measurable activity following the end of irradiation.

The selection of wires and foils is governed by a series of American Society of Testing and Materials (ASTM) standards that utilize the International Reactor Dosimetry and Fusion File (IRDFF) cross section database.

During the selection and fabrication process, the total mass of each foil and wire is constrained based on predicted neutron spectra and irradiation characteristics to provide measurable gamma-ray emissions while maintaining a low dose rate for personnel during removal and handling of the capsules from the reactor or experiment. Wires or foils are often encapsulated in vanadium canisters, due to the low attenuation of neutrons through vanadium, that afford a physical barrier for dosimetry materials so as to prevent oxidation and contain prevent leakage of melted materials, if necessary.

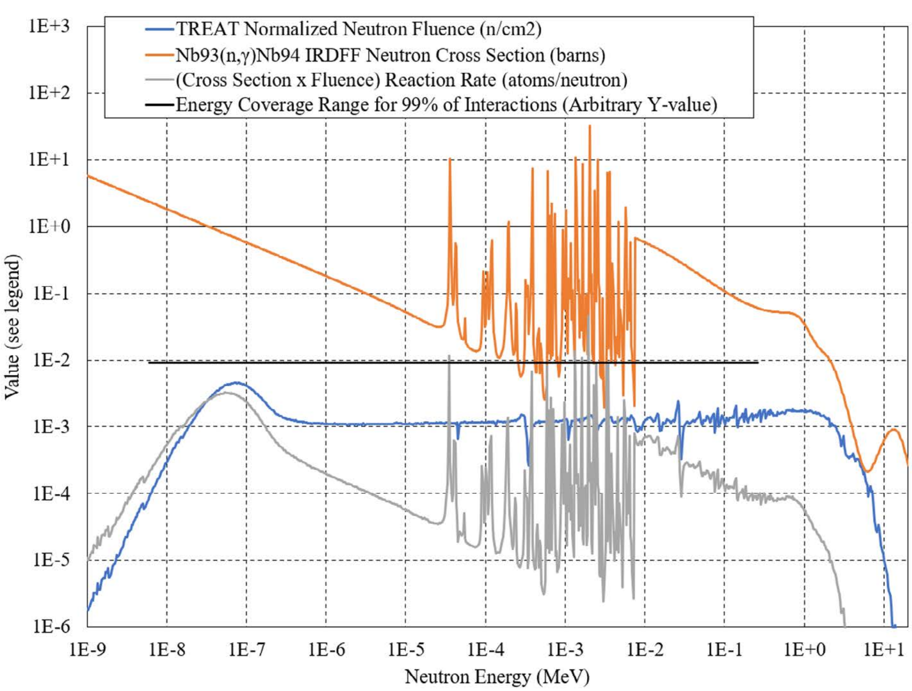

Figure 7. Normalized TREAT neutron fluence (blue) compared with 93Nb(n,γ)94Nb cross section (orange), reaction rate (gray), and energy range that incorporates 99% of interactions (black).

Following irradiation, the activated materials are brought to the INL Research Complex (IRC) Reactor Metrology laboratory, where they are measured with a high-purity germanium (HPGe) detector. The HPGe detector is well-characterized and identifies the radioisotopes created during irradiation. By comparing the activities of the radioisotopes against the measured masses of the initial foils or wires, the reaction rate for each reaction can be determined.

Ideally, all useful materials for the irradiation within the IRDFF library would be incorporated. However, this would typically include more than 20 dosimetry materials and may preclude the inclusion of an experiment capsule.

Continued on next page

Continued from previous page

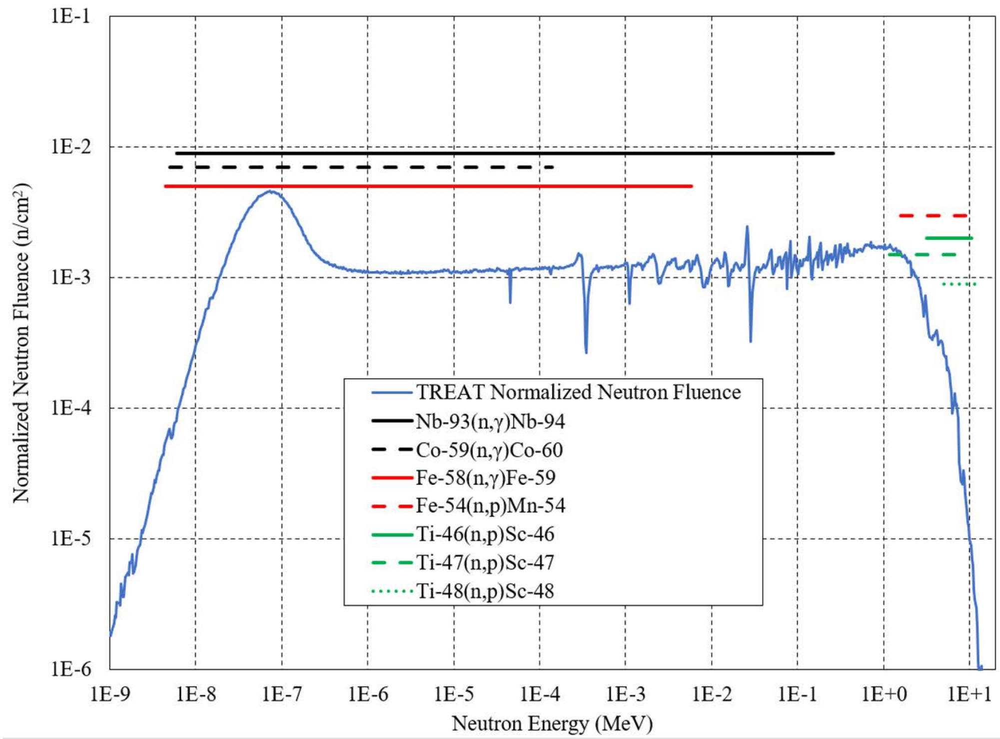

Figure 8. Normalized TREAT neutron fluence (blue) compared against energy coverage ranges for a selection of materials.

Instead, our team optimizes the choice of materials based on each experiment's unique irradiation characteristics and geometry restrictions to provide as many unique "energy coverage ranges" as possible.

In Figure 7, the simulated energy-dependent neutron fluence for the Transient Reactor Test (TREAT) facility is shown in blue with 1000 energy groups. The cross section for the absorption of a neutron by ^{93}Nb to produce ^{94}Nb is shown in orange. By multiplying the cross section (orange) by the neutron fluence (blue), an energy-dependent reaction rate is determined (gray). The magnitude of the gray data points provide insight for neutron energies to which $^{93}Nb(n,\gamma)^{94}Nb$ is sensitive, and 99% of the reactions occur in the "energy coverage range" of the black line shown.

In Figure 8, a selection of energy coverage ranges is shown for the TREAT neutron spectrum for common dosimetry materials. The variety of coverage ranges provides experimenters, including the ASI program, with reaction rates of specific dosimetry materials, as well as the ability to quantify the magnitude and profile of the neutron spectrum so as to inform characterization of the irradiation cavity or irradiation environment that provided neutrons to the irradiation experiment.

Sparse Sensing and Sparse Learning for Nuclear Digital Twins

Mohammad G. Abdo
Idaho National Laboratory

Introduction

Nuclear power plants lack the luxury of the immersive sensing required for continuous monitoring of various systems, structures, and components to ensure safe and efficient operations. Accurate reconstruction of fields of interest (e.g., temperature, pressure, velocity, etc.) from sensor measurements is crucial to establish a two-way communication between physical experiments and models. However, deploying extensive sensor arrays in nuclear reactors is infeasible due to challenging operating conditions and inherent spatial limitations. To address this, the team at INL and the collaborators at University of Washington have developed a data-driven technique that integrates constraints into an optimization framework for sensor placement, aiming to minimize reconstruction errors under noisy sensor conditions. This method was validated using the out-of-pile Testing and Instrumentation Transient Water Irradiation System (OPTI-TWIST) prototype capsule, which emulates the neutronic effects of nuclear fuel through electrical heating. The prototype, intended for insertion in INL's Transient Reactor Test Facility (TREAT), provides a practical demonstration of our approach. Additionally, the technique was applied to a tri-structural isotropic (TRISO) fuel irradiation experiment and a steam generator, demonstrating how optimized sensor placement can accurately reconstruct fields of interest. The results show minimized reconstruction errors, probabilistic bounds for noise-induced uncertainty, and establish effective communication between digital twins and experimental facilities or physical assets. For nuclear applications, where sensor deployment is limited, optimal sensor placement is crucial. Machine learning algorithms can leverage sparse sensor data to accurately reconstruct full fields of interest, classify accident scenarios, and predict their occurrence faster than real-time.

Case Study 1. Out-of-Pile Testing and Instrumentation Transient Water Irradiation System (OPTI-TWIST) prototype capsule:

This capsule is electrically heated to emulate the neutronic effect of the nuclear fuel. The TWIST prototype that will eventually be inserted in the Transient Reactor Test Facility (TREAT) at the Idaho National Laboratory (INL). The resulting sensor-based temperature reconstruction within OPTI-TWIST demonstrates minimized reconstruction errors, provides probabilistic bounds for noise-induced uncertainty, and establishes a foundation for communication between the digital twin and the experimental facility.

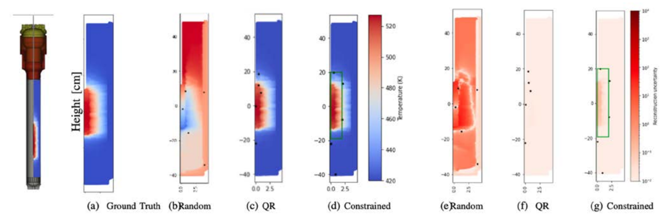

Figure 9. OPTI-TWIST temperature Reconstruction.

Case Study 2. TRISO Fuel Irradiation Experiment:

A graphite holder for the annular TRISO fuel came with a large number of bores that were down selected by the algorithm so as to only require placement of three thermocouples. The associated depth was decided such

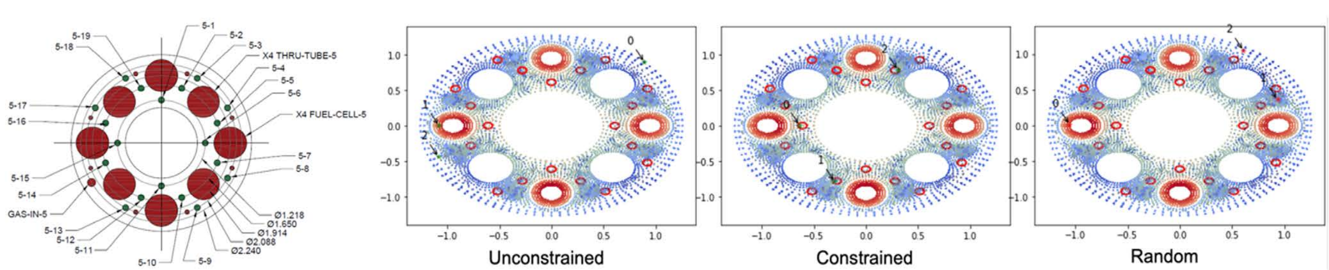

Figure 10. Graphite holder for the TRISO irradiation experiment.

Continued on next page

Continued from previous page

that the 3D temperature field is reconstructed at BOC and at end of cycle (EOC) for each power perturbation. The accuracy outperformed any random placement. The maximum error recorded did not exceed 2%.

Sensor	X	Y	Z	Sensor	X	Y	Z	Sensor	X	Y	Z
0	0.892	0.892	12.3080	0	-0.638	0.005	9.000	0	-1.050	0.110	11.346
1	-1.081	0.000	14.1535	1	-0.302	-0.781	11.154	1	0.857	0.252	14.000
2	-1.088	-0.438	9.8000	2	0.306	0.783	14.167	2	+0.615	0.892	10.962

Table 1. Sensor locations pertaining to the optimal unconstrained case, being constrained to the holes, and random placement respectively

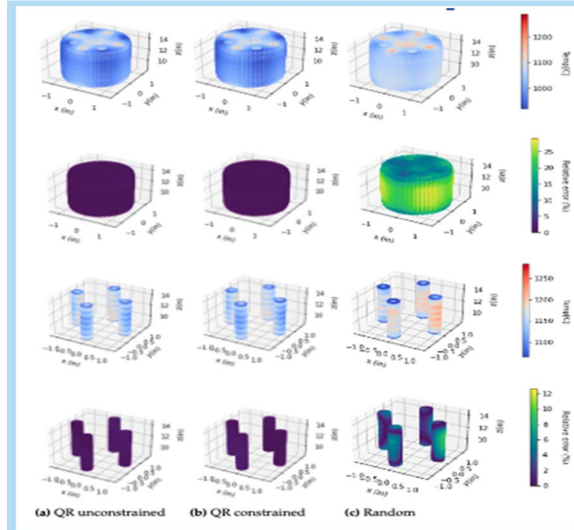

Figure 11. Holder field reconstruction, relative error, fuel temperature reconstruction, and relative error (Top to Bottom).

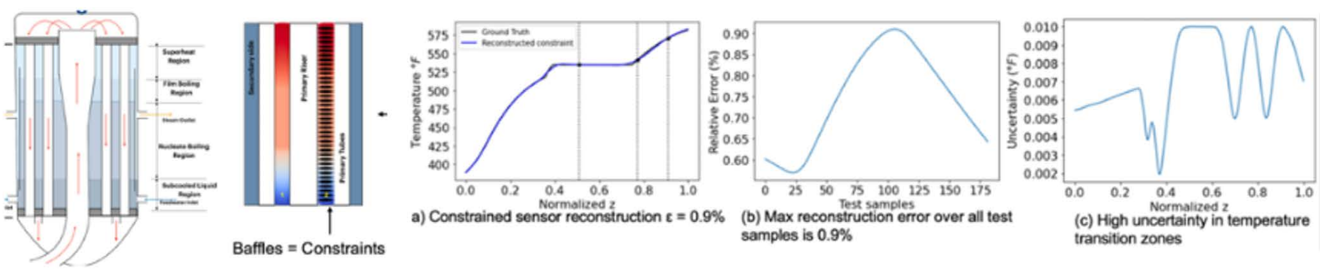

Figure 12. Steam generator design and temperature field reconstruction with the associated error and spatial uncertainty respectively.

Case Study 3. Steam generator Design:

In this case study, a 1D simulation of a steam generator that used several empirical equations for different boiling mechanisms was used along the height of the steam generator which was treated as a black box. The algorithm was able to reconstruct several fields of interest including temperature, flux, and velocity. The maximum error was below 1% and the modes of the reduced order model revealed the normalized heights separating each boiling mechanism, as confirmed by the designers.

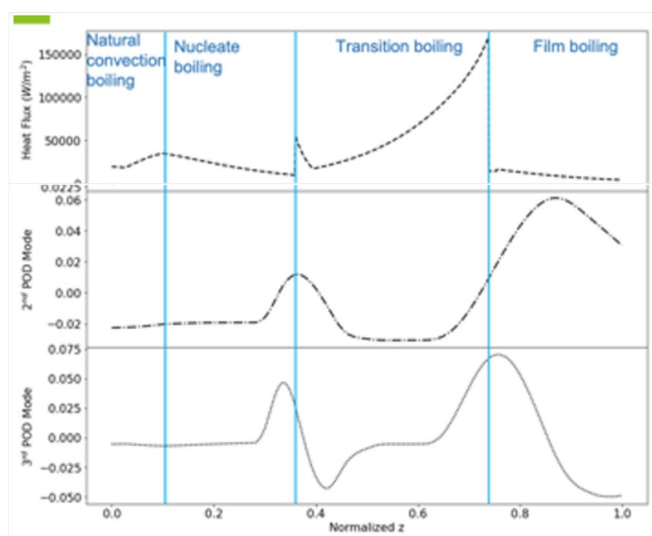

Figure 13. Reduced order model revealing interfaces between boiling mechanisms confirmed by the designer.

Innovative Monitoring Technology Coupling Sparsely Spaced Sensors and Machine Learning

Lesley Wright
Texas A&M University

Elia Merzari
Pennsylvania State University

Roberto Ponciroli
Argonne National Laboratory

Lander Ibarra
Argonne National Laboratory

Introduction

Commercial nuclear power plants encounter significant financial setbacks due to prolonged downtimes required for maintaining the most expensive components of the nuclear island. In the case of reactor containment vessels, surface degradation occurs over time due to thermo-mechanical fatigue, embrittlement, and/or corrosion, ultimately compromising their structural integrity and necessitating replacement. This economic hurdle inevitably diminishes the attractiveness of adopting nuclear energy. However, the implementation of a real-time monitoring system for assessing the vessel's health can enable plant operators to proactively schedule maintenance, thus significantly reducing downtime.

To be economically competitive in deregulated energy markets, microreactors need to adopt novel operational paradigms. Some are being designed to assume new roles within the power grid, offering enhanced flexibility compared to past designs and/or relying on passive cooling approaches that subject the reactor vessel to more demanding duty cycles. Over a reactor's lifetime, these operational modes can lead to an increase in mechanical loads on the reactor pressure walls and compromise its integrity.

This team of researchers is leveraging recent advances in both machine learning (ML) based field reconstruction techniques and diagnostic software to augment traditional sensor capabilities. We have demonstrated an integrated sensor technology for real-time monitoring of thermal-mechanical stresses of the reactor vessel of micro-high temperature gas reactors (mHTGRs). The technology provides (1) a real-time, reliable and cost-effective monitoring methodology, (2) a quantification of the lifetime and integrity of the pressure vessel of the mHTGR, and (3) a means to improve the economics of the microreactor systems.

Impact

For monitoring reactor vessel conditions in harsh environments, two strategies are available: (1) developing new sensors or (2) designing advanced algorithms that leverage existing sensors placed in locations where their performance would not rapidly degrade. These approaches can be pursued independently or in a complementary manner. The team has developed and began demonstrating a real-time monitoring system for mHTGR reactor pressure vessels using commercially available strain and temperature sensors. Commercially available sensors can be placed on the outside of the vessel, providing economic and robust monitoring. The output from the sensors is coupled with numerical predictions and machine learning to reconstruct the thermal-mechanical behavior throughout the vessel wall (both internally and externally).

A 1:23 scaled vessel facility was constructed to simulate the monitoring system of an actual HTGR reactor vessel. This vessel setup can be heated to 650°C, using 3 radiant heaters. The temperature field on the vessel is obtained by an array of 32 thermocouples that are welded to the surface. Next, an array of strain gauges was mounted on the vessel to provide real-time strain measurements. The strain was measured under various heating conditions, including off-operating conditions. Figure 14 shows the gauges successfully captured the critical event, without penetration into the vessel. Furthermore, the thermal-mechanical measurements provide a foundation for validation of numerical simulations.

Building on the experimental work, a Convolutional Neural Network (CNN) for field reconstruction was used to predict the temperature distribution induced by radiative heaters over a convex metal surface representing a section of the mHTGR vessel wall. This temperature distribution was later used to evaluate the thermal-induced strain over that domain. We successfully created a computational model capable of reproducing the experimental results.

We trained our network using two datasets to evaluate its ability to reconstruct off-normal operational cases without prior exposure. It could predict the temperature distribution over the entire vessel wall using eight out of the 32 available thermocouples measures with a temperature deviation smaller than 50 K when

Continued on next page

Continued from previous page

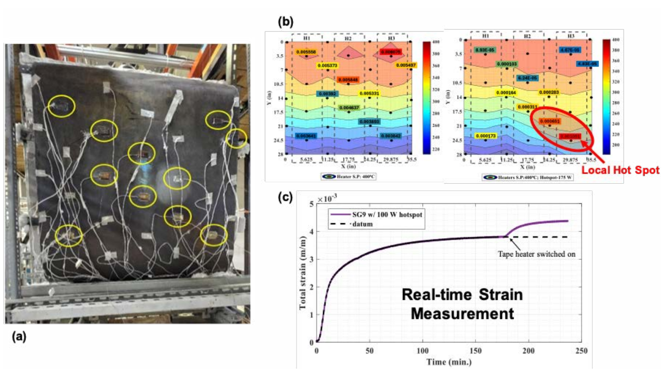

Figure 14. Laboratory Model of a Vessel Reactor Wall for Thermal-Mechanical Measurements (32 Thermocouples and 11 Strain Gauges) (a) Photograph of the Instrumented Vessel Wall; (b) Temperature and Strain Distributions for "Normal" and "Incident" Conditions; (c) Real-Time Strain Measurements Indicating when the Hot Spot was Detected by a Nearby Strain Gauge

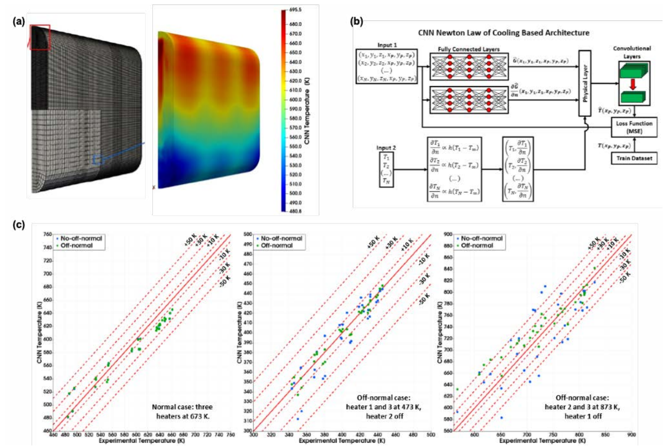

Figure 15. Reconstruction of the Vessel Temperature Field from the CNN (a) Sample Computational Model and Detailed Temperature Field Reconstruction; (b) CNN Architecture Coupling Radiative and Convective Heat Transfer; (c) Comparison of Local Temperatures Predicted by the CNN against Experimental Measurements for both Design and Off-Design Conditions

adding off-normal cases into the training dataset. Excluding off-normal cases from the training dataset results in significant uncertainties in temperature field reconstruction. We demonstrated the ability to reconstruct the temperature field distribution over the HTGR vessel wall using experimental data as input for the CNN, marking it as the first validation of this architecture, and we achieved a maximum relative error of 11.6% over all test cases analyzed. Using the temperature distribution predicted by the CNN and the MOOSE computational model, we were able to estimate the thermal-induced strain over the vessel wall. This is the first demonstration to our knowledge of the use of thermocouples to evaluate strain.

Future Work

The results presented in this work highlight the applicability of the methodology introduced as a powerful tool in predictive maintenance problems, allowing us to estimate the thermal-induced stress and strain with a few readings from commercially available sensors. Based on the CNN's performance for off-design conditions, we have identified areas of improvement for the network. This work has enabled us to extend the network beyond its initial capabilities, and we will continue refining it to enhance the characterization and prediction of various incident scenarios while minimizing the need for extensive training data. With the framework developed and demonstrated over a range of operating conditions, future studies will involve sensor placement optimization. Using the recently developed predictive capabilities, the number of sensors can be minimized to both effectively and economically monitor reactor component operation.

Field-Assisted Embedding of Fiber Bragg Gratings with Compressive Strain for Sensing at High Temperatures

Xinchang Zhang
Idaho National Laboratory

Jorgen Rufner
Idaho National Laboratory

Joshua Daw
Idaho National Laboratory

Charles Payne
Idaho National Laboratory

Bibo Zhong
Idaho National Laboratory

Austin Fleming
Idaho National Laboratory






Introduction

Embedded fiber optic sensors are gaining significant interest as strain and temperature sensors for structural health monitoring (SHM) in various industries [1-3]. A network of embedded fiber optic sensors, such as fiber Bragg gratings (FBGs), enables real-time and distributed sensing of critical parameters, offering valuable insights into temperature, strain, stress, and potential failure points to assess structural integrity. The use of smart materials with embedded FBGs holds great promise across industries such as nuclear, aerospace, and oil and gas. Fiber optic sensors possess intrinsic properties that make them well-suited for SHM in extreme nuclear environments, including both fission and fusion systems. The successful integration of fiber optic sensors into structural materials necessitates effective interfacial bonding between the fiber and matrix, good integrity and functionality of the embedded sensors, robust mechanical strength of the matrix materials, and the ability to retain these properties during transient thermal and stress events. Previous work by our team has successfully demonstrated the embedding of fiber optic sensors with these essential properties [4, 5]. Furthermore, it is critical to ensure that sensors embedded in host metallic structures can operate at high temperatures (~1000°C), where they face stress from the mismatch in the coefficient of thermal expansion (CTE) between fused silica fiber and metals such as stainless steel and nickel alloys. Solutions to maintain sensor functionality at elevated temperatures include sensor-matrix strain isolation and pre-compression of the embedded fibers [6]. While the former is suitable for temperature sensing, it is not feasible for strain measurements due to sensor-matrix strain uncoupling. The latter (pre-compression), however, is critical when strain sensing is the primary objective. This study demonstrates the embedding of FBGs in structural materials, achieving compressive strain on the fibers to compensate for thermal strain caused by CTE mismatch at high temperatures. This study demonstrates temperature sensing at up to 900°C, using the embedded FBGs with precompressed strain, as fabricated via the developed advanced manufacturing technology.

Methodology

This study demonstrates the use of electric-field-assisted sintering (EFAS) to embed FBGs in metallic materials (i.e., SS-316L and nickel) for sensing applications. EFAS leverages electric current and pressure to rapidly synthesize materials (metals, ceramics, and composites) using significantly less energy than traditional pressing and sintering techniques. Key EFAS parameters, such as temperature, pressure, and time, can be adjusted to control the microstructure, residual stress, and other properties of the processed materials. Employing EFAS technology and advanced characterization and testing tools, our team has demonstrated successful embedding of fused silica optical fibers and sapphire fibers in SS316L and nickel matrix earlier [4, 5, 7]. The current study advances these sensor embedding capabilities by achieving compressive strain/stress on the embedded fibers, ensuring their survivability at high temperatures (~1000°C). In this work, FBGs were embedded in SS316L and nickel using EFAS under different fabrication conditions, and the resulting compressive strain on the embedded FBGs was measured. The effect of EFAS parameters on the state of compressive strain was investigated. These embedded FBGs were tested at up to 900°C, and the strain evolution was analyzed by monitoring shifts in reflected wavelength of the FBGs.

Continued on next page

Continued from previous page

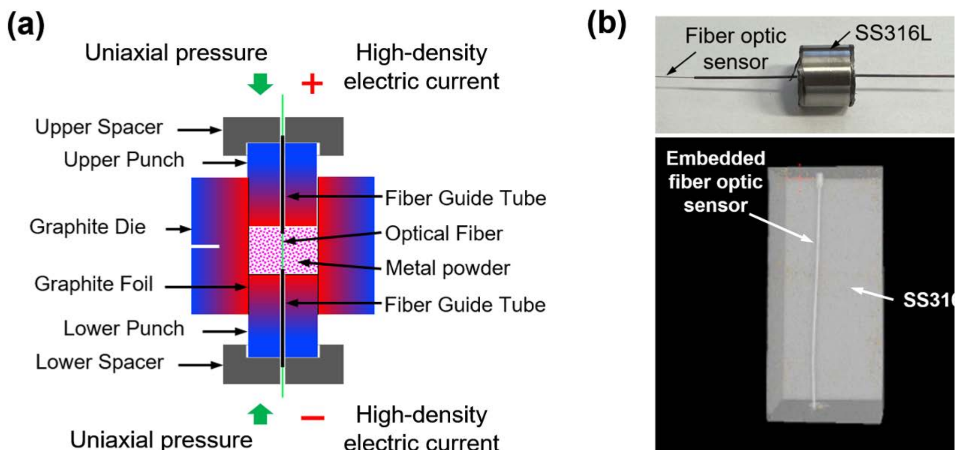

Figure 16. (a) Schematic representation of the embedding process using EFAS. (b) SS316L part with embedded fibers and X-ray computed tomography scan of the part

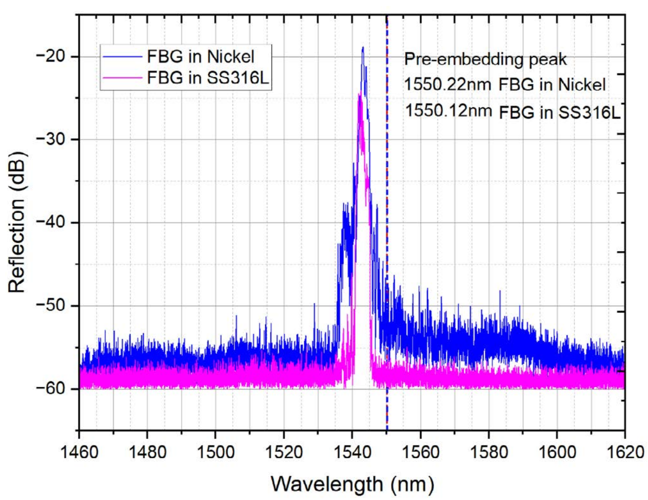

Figure 17. Reflection spectrums of FBGs embedded in SS316L and nickel fabricated at 600°C measured at room temperature.

Figure 16 illustrates the embedding process using EFAS. Commercially available single-mode FBGs, obtained from Technica Optical Components, LLC, were used in this study. These FBGs have an inscribed wavelength of ~1550 nm over a 5-mm length. As shown in Figure 16, the FBG was placed into a graphite mold, which was then filled with metal powders (SS316L and nickel). The powder-sensor compacts were sintered via EFAS at 600°C and 900°C under an applied pressure of 10 and 40 MPa, with a 5-minute dwell at the sintering temperatures. Figure 16b shows a fabricated part, along with an x-ray computer tomography scan of it, revealing the fiber within the matrix.The reflective wavelengths of the FBGs, embedded at different EFAS conditions, were measured using a Luna optical sensing instrument. Figure 17 shows the room-temperature (RT) reflection spectrum of the FBGs embedded in SS316L and nickel at 600°C. At RT, compressive strains of 3768 με and 3683 με were measured from the FBGs embedded in nickel and SS316L, respectively. For the FBG embedded in SS316L fabricated at 900°C, a compressive strain of 11,574 με was measured at RT. These results demonstrate that compressive strain was successfully achieved in the embedded FBGs, and the embedding parameters significantly influence the strain conditions. Specifically, increasing fabrication temperature and pressure led to a higher compressive strain in the FBGs.

The embedded FBGs were tested in a furnace at high temperatures, with their reflective spectra being recorded in-situ to monitor strain evolution. Figures 18a and 18b show the testing of the FBG embedded in nickel (fabricated via EFAS at 600°C) up to 700°C and 900°C, respectively. The results demonstrate the successful response of the FBG sensor to temperature changes. As the temperature increased, the strain gradually transitioned from compressive to tensile. The FBGs survived the testing at 900°C, with a peak tensile strain of ~6,300 με at 900°C. These results highlight that the pre-compression applied to the FBG during embedding ensures the sensor's integrity at high temperatures, enabling its use in high temperature applications.

Figures 19a and 19b show the testing of the FBG embedded in SS316L (fabricated at 900°C) up to 700°C and 900°C, respectively. The embedded FBG also survived these tests. As the temperature increased, the strain transitioned from compression to tensile. Since this FBG has high compressive strain at RT having been embedded at a higher temperature (900°C), a peak tensile strain of ~6,000 με was measured at the testing temperature of 900°C. The successful testing of FBGs embedded in both nickel and SS316L demonstrates the advantages of EFAS technology for embedding fiber optic sensors into high-temperature structural materials to obtain pre-compressive stress/stress on sensors for SHM at high temperatures.

Continued on next page

Continued from previous page

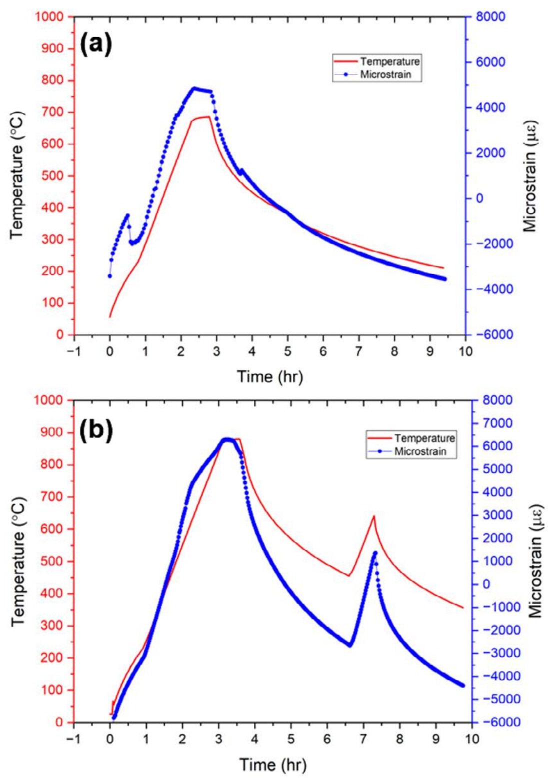

Figure 18. Evolution of FBG strain as a function of temperature up to (a) 700°C and (b) 900°C for the FBG embedded in nickel.

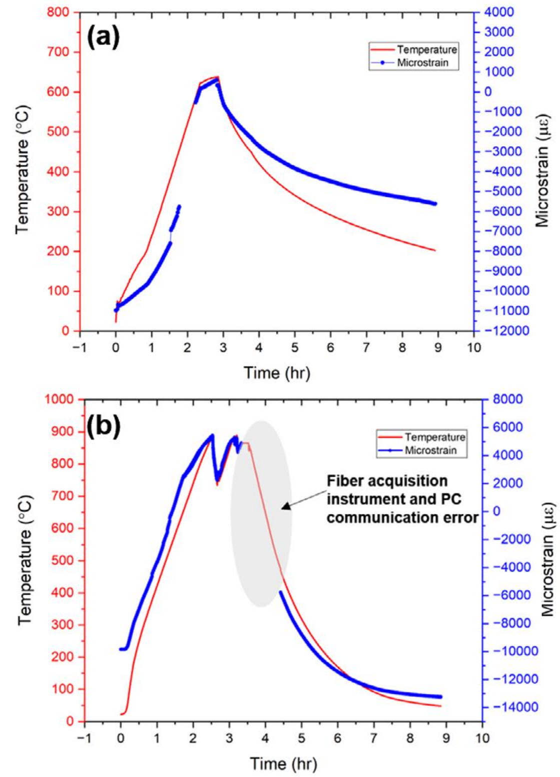

Figure 19. Evolution of FBG strain as a function of temperature up to (a) 700°C and (b) 900°C for the FBG embedded in SS316L.

Impact

Incorporating fiber optic sensors into nuclear components offers significant potential to enhance the safety, efficiency, and operational longevity of nuclear systems. These sensors have been widely used in both nuclear and non-nuclear fields for structural health monitoring and autonomous controls. Embedding them in materials for use in harsh environments is highly desired. Therefore, this study, by demonstrating the sensor performance, enables the measurement of real-time, distributed data across various structures and facilitating integration with central monitoring systems. By leveraging these sensors, operators gain a comprehensive view of critical parameters along the length of the fiber, which helps detect early signs of structural degradation, cracks, or deformation. This, in turn, supports better situational awareness and decision-making, improving both operational efficiency and safety. This capability is especially valuable for nuclear systems deployed at remote locations or space, such as small modular reactors and microreactors. The integration of embedded fiber optic sensors with advanced control systems enables remote monitoring and control, paving the way for the development of smart sensor networks for a wide range of applications.

References

[1] H.C. Hyer, D.R. Giuliano, C.M. Petrie, Toward local core outlet temperature monitoring in gas-cooled nuclear reactors using distributed fiber-optic temperature sensors, Applied Thermal Engineering 230 (2023) 120847.

[2] R. Di Sante, Fibre Optic Sensors for Structural Health Monitoring of Aircraft Composite Structures: Recent Advances and Applications, Sensors 15(8) (2015) 18666-18713.

[3] H.M. Hashemian, W.C. Bean, Sensors for Next-Generation Nuclear Plants: Fiber-Optic and Wireless, Nuclear Science and Engineering 169(3) (2011) 262-278.

[4] X. Zhang, Z. Hua, C.A. Picklesimer, W.C. Chuirazzi, C. Sun, M.D. McMurtrey, J. Rufner, Integrating fiber optic sensors into metallic components for sensing in harsh environments, Optics & Laser Technology 170 (2024) 110188.

[5] X. Zhang, J. Daw, C. Payne, B. Zhong, A. Fleming, Z. Hua, J. Rufner, Electric field-assisted embedding of fiber optic sensors in structural materials for structural health monitoring, Journal of Materials Research and Technology 34 (2025) 15-31.

[6] J. Mathew, A method of attaining optical fibre pre-compression for strain and temperature monitoring inside metal at extremely high temperatures, Sensors and Actuators A: Physical 379 (2024) 116000.

[7] X. Zhang, Z. Hua, J.F. Rufner, Smart Structural Materials With Embedded Fiber Optic Sensors for Health Monitoring in Harsh Environments, ASME 2023 Conference on Smart Materials, Adaptive Structures and Intelligent Systems, 2023.

High Temperature Magnetostrictive EMAT Sensors for Advanced Reactors

Bill Glass
Pacific Northwest National Laboratory

Morris Good
Pacific Northwest National Laboratory

Nicholas Conway
Pacific NorthwestNational Laboratory

Tianhao Wang
Pacific Northwest National Laboratory

The Department of Energy's Advanced Sensors and Instrumentation program seeks to develop and qualify advanced sensors for the nuclear industry. Periodic inspection technology such as conventional manual or manually installed robotic technology will not be possible for most planned advanced reactors. Long duration operating cycles and high radiation levels will limit or exclude personnel access. Reliable high temperature and high radiation sensors for online monitoring of pipes, vessels, and other critical components for cracks, pitting, and other flaws will be highly desirable or essential for license justification and to aid in operation for the advanced reactors and may also serve to improve safety margins for conventional light water reactors. Current light water reactors have a coolant T-hot approaching 350°C; liquid sodium reactors range from 350°C to 550°C or higher; and molten salt reactors operate at >700°C. Currently, no suitable sensors exist for monitoring the structural integrity of any of these reactor designs.

Magnetostrictive Electromagnetic Acoustic Transducers (EMATs) using a cold spray cobalt coating have emerged as a promising solution. These sensors could potentially endure long term exposure to extreme temperatures and provide online monitoring capabilities to detect cracks, pits, and erosion/corrosion damage before these flaws lead to through-wall failures.

The research team at PNNL, consisting of Bill Glass, Morris Good, Nicholas Conway, and Tianhao Wang, has chosen cold spray cobalt (Co) for a magnetostrictive EMAT designed for high temperature service. Bill, Morris, and Nicholas bring decades of experience with ultrasound and EMAT sensors, while Tianhao contributes his expertise in microscopy and X-ray diffraction to understand the interaction between microstructure and sensor performance.

Magnetostrictive sensors operate on the principle that a change in the magnetic field induces a change in the shape of a magnetostrictive material. EMAT sensors consist of a biasing magnet and a coil that perturbs the magnetic bias field when subjected to a high current pulse. The magnetostrictive material deformation generates an ultrasound-guided stress wave that can propagate through a large volume of material that can then be inspected for material discontinuities and flaws, making them a valuable tool for non-destructive testing. Traditional piezoelectric sensors used for ultrasound inspections are limited to approximately 250°C due to the temperature constraints of the active piezoelectric crystals and mechanical coupling. In contrast, EMATs can be constructed from materials that withstand higher temperatures, and their inductive non-contact coupling overcomes the piezoelectric limitations of direct mechanical contact coupling. Two versions of the EMAT were investigated:

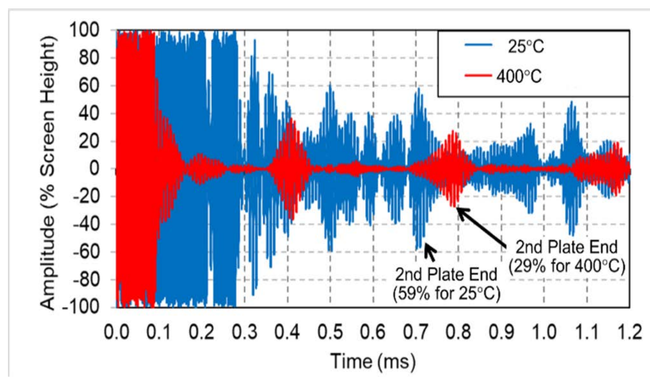

Figure 20. AlNiCo permanent magnet response at 25°C and 400°C showing the 2nd plate end reflection at 400°C to be 29% of 25°C response.

1. A permanent magnet version based on an AlNiCo magnet that can withstand temperatures exceeding 400°C and does not require a high current, high-temperature wire coil to create the bias magnetic field (figure 20).
2. An electromagnet version that can generate a magnetic bias field at temperatures exceeding 800°C, albeit with challenges related to managing additional high-temperature wires (figure 21).

The cold spray cobalt coating serves as the magnetostrictive element of the sensor. Despite the surprising and significantly non-linear thermal response of cold spray cobalt, it maintained a magnetostrictive

Continued on next page

Continued from previous page

response greater than 20% of the room temperature response even at the highest temperatures tested (figure 22). The PNNL team successfully demonstrated the EMAT's ultrasound response to features of interest using the permanent magnet version up to 400°C and the electromagnet version up to 889°C.

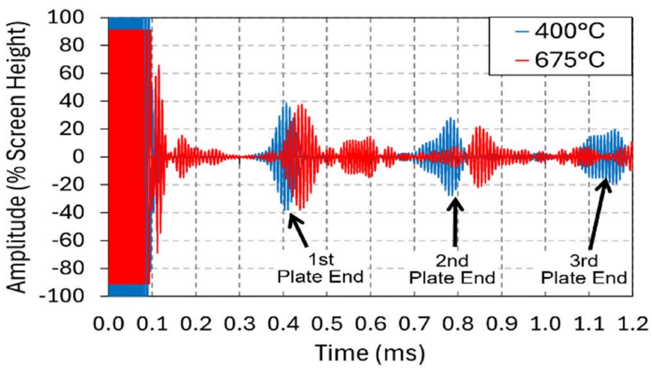

Figure 21. Electromagnet 400 and 675°C responses show clear plate end reflections. Responses at some temperatures were clearer than others.

This magnetostrictive EMAT advancement significantly enhances the potential for online monitoring of high-temperature reactor components. Such a capability supports both licensing and operation safety by enabling online high temperature monitoring to detect cracks

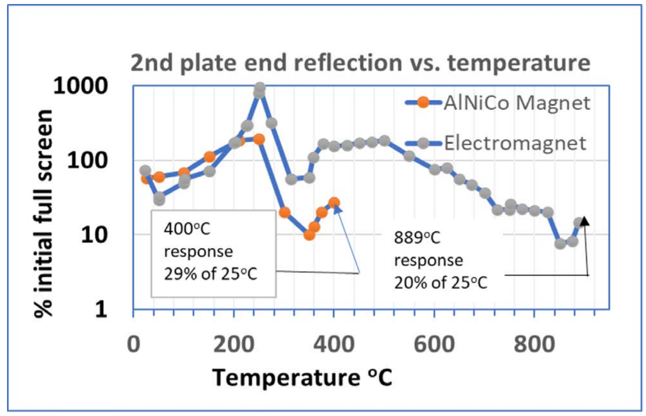

Figure 22. Cold sprayed Cobalt Magnetostrictive EMAT with both AlNiCo permanent magnet response at 400°C and electromagnet response to 850°C were above 20% of 25°C responses.

and flaws before they progress to through-wall leaks or structural failures. Early detection and monitoring of growing flaws allows mitigation and repair before a safety significant event occurs.

Continued work is planned for other magnetostrictive materials like FeCo and Galfenol which may have a more monotonic temperature response and also may not be subject to Co-59 (Co's naturally occurring stable isotope) transformation to the more radioactive Co-60 in the presence of neutron radiation.

For more information, contact Bill.Glass@pnnl.gov

Langasite Surface Acoustic Wave Sensors for High Temperature Nuclear Reactor Monitoring Applications

Luke Doucette
University of Maine

Morton Greenslit
University of Maine

Mauricio Pereira da Cunha
University of Maine

Introduction

There is a significant need for harsh environment sensor materials and sensor systems that can provide reliable, long-term structural health monitoring (SHM) and prognostic capabilities for advanced micro-reactors and high temperature gas reactors (HTGRs) [1],[2]. In addition to being tolerant to high gamma radiation (e.g., > 10 Gy/s) and neutron flux levels (> 10^{12} n/(cm^2·s)), in-core sensors must also be able to withstand the high operating temperatures (> 700°C) that are typically required to achieve the desired high energy conversion efficiencies for these reactors. Such harsh environment constraints limit the type and number of sensor technologies that can be successfully implemented in these reactor systems. For example, there is currently a lack of commercially available in-core neutron flux sensors that can reliably function at temperatures above 550°C [2].

To address these sensor needs for high temperature advanced reactors, researchers at the University of Maine recently demonstrated a langasite (LGS)-based surface acoustic wave resonator (SAWR) sensor technology that is capable of measuring total neutron flux levels up to 2×10^{12} n/(cm^2·s) while operating at 800°C [3]. The SAWR sensor frequency responses were measured in-situ during irradiation exposure and under high temperature conditions at the Ohio State University Nuclear Reactor Laboratory (OSU-NRL) facilities, and supported by the Nuclear Science User Facilities (NSUF) program. The effects of gamma heating on SAWR sensor frequency responses were accounted for by using a controlled furnace that kept the SAWR sensors at a fixed high temperature when exposed to different reactor powers/neutron flux levels. The measured variations in sensor frequency responses could then be primarily attributed to neutron flux induced material softening of the SAWR devices' elastic moduli [4],[5]. As such, this material softening produced frequency variations at a rate of approximately 3 kHz per 0.4×10^{12} n/(cm^2·s), or per 100 kW of reactor power, while operating at 800°C.

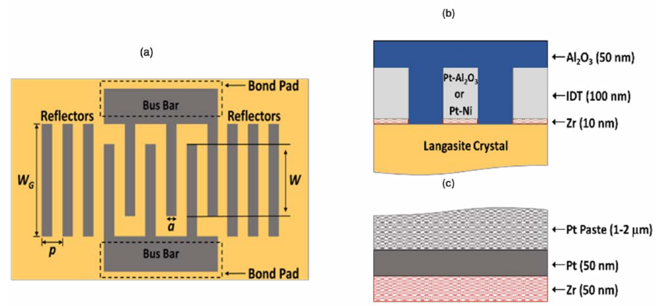

Fig. 23. (a) Top-view schematic of the SAWR sensor device. (b) Cross section of the device at the electrode region. (c) Cross section of the bond pad electrode on top of the bus bar region used for field coupling to the bus bars/interdigital transducer electrodes. Reproduced from [3].

Sensor Fabrication and Packaging

For the work described here, a total of seven LGS SAWR sensors were designed, fabricated, packaged, and calibrated for high temperature operation using UMaine cleanroom fabrication and sensor testing facilities, and were characterized under nuclear radiation and high temperature conditions at OSU-NRL. Fig. 23a-c shows a top-view and side profile diagrams of the general SAWR layout and thin film stack utilized in this work. Five of the devices were fabricated with co-deposited $Pt-Al_2O_3$ electrodes, and two of the devices were fabricated with alloyed Pt-Ni electrodes, both of which were nominally 100 nm thick. The $Pt-Al_2O_3$ and Pt-Ni electrode-based SAWRs operated at 331 MHz and 285 MHz resonant frequencies, respectively. These electrode configurations were chosen due to their known stability when operated at temperatures up to the 800°C to 1000°C range under prior testing [6],[7]. In addition, the testing of SAWR sensors with different high-temperature electrode materials ($Pt-Al_2O_3$ and Pt-Ni) enabled investigations on the influence of material-dependent irradiation softening for the different electrodes, which can impact the overall sensor sensitivity under different reactor power levels and high temperature conditions.

Fig. 24a shows a fabricated LGS SAWR sensor mounted and electronically connected to a high-temperature Inconel coaxial cable using 4 mil and 1 mil platinum (Pt) bond wire, respectively. To further protect the exposed SAWR sensors during transport and testing at OSU-NRL,

Continued on next page

Continued from previous page

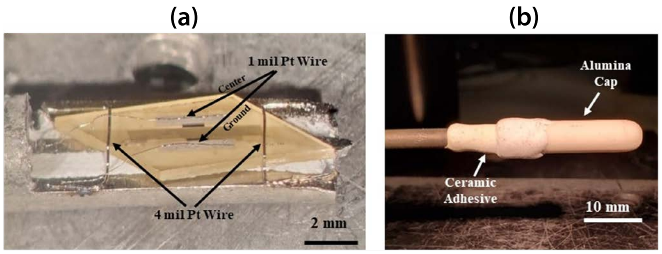

Fig. 24. (a) Top-view of a LGS SAWR sensor device attached and electronically connected to a high temperature Inconel cable. (b) The same device shown in (a) packaged/protected with an alumina cap using a high temperature ceramic adhesive. Reproduced from [3].

high temperature alumina caps were used to cover and package the sensors as shown in Fig. 24b. These UMaine developed wire bonding and device packaging techniques have been successfully tested under a variety of high temperatures and harsh environments [8], and are a critical aspect for successful SAWR sensor testing in advanced high temperature reactors.

High Temperature Reactor Facility Used for Sensor Testing

Fig. 25 shows the OSU-NRL high-temperature test rig furnace and the pool-based reactor facility utilized in this work for in-situ monitoring of the LGS SAWR frequency responses as a function of reactor power/neutron flux and high temperature. The fabricated sensor probes shown in Fig. 24 were initially inserted into the furnace (Fig.25a), which is capable of maintaining fixed high temperatures. Once loaded into the furnace, the sensors were then connected to low temperature RF coaxial cables that were externally routed to a data acquisition system for obtaining in-situ sensor measurements. Two separate type-K thermocouples were included with the sensor bundle and positioned immediately next to the sensors for local temperature measurement feedback. Once the seven SAWR sensors were installed into the furnace, the entire rig shown in Fig. 25a was lowered into a movable vertical ex-core steel dry tube shown in Fig. 25b and positioned next to the reactor core as shown in Fig. 25c.

High temperature irradiation testing of the LGS SAWR sensors took place over five days at OSU-NRL. During this test period, all seven sensors were exposed to a total neutron fluence of approximately 10^{17} n/cm^2; and maximum neutron and gamma flux rates of 2×10^{12} n/(cm^2·s) and 21 Gy/s, respectively, which occurred at the reactor's maximum power of 461 kW. The test temperatures ranged from room temperature to a maximum of 800°C during irradiation.

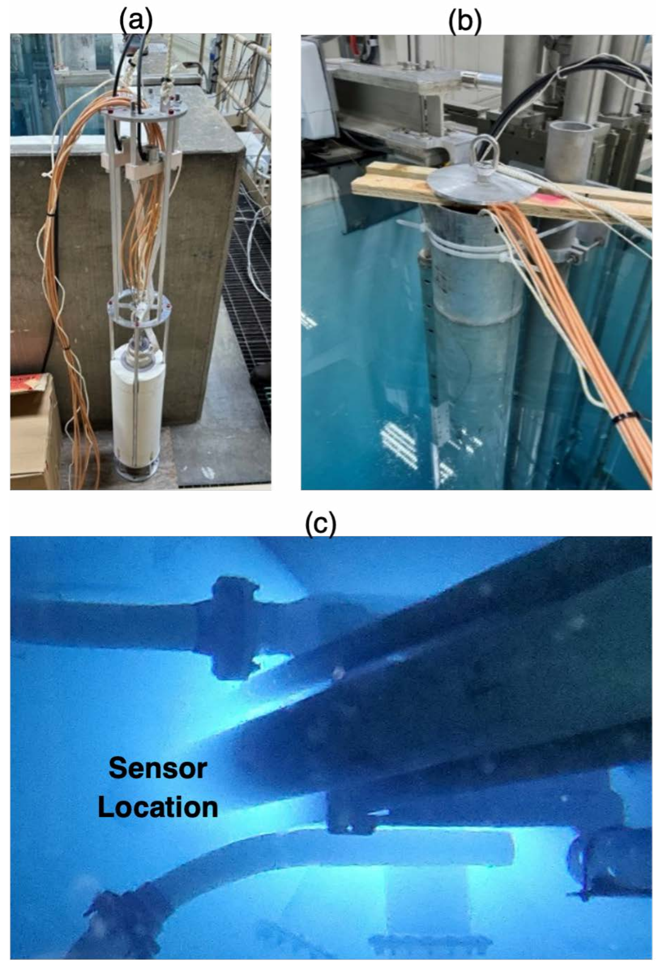

Fig. 25. (a) High temperature test rig loaded with a set of seven LGS SAWR sensor probes. (b) Vertical steel dry tube in the reactor pool, showing low temperature RF cables extending from the tube. The RF cables connect the sensor probes located in the furnace at the bottom of the dry tube to a DAQ system located on a nearby benchtop for in-situ sensor monitoring. (c) A view looking down into the reactor pool during high temperature / high irradiation LGS SAWR sensor testing. Reproduced from [3]

Current Status and Highlights

All seven LGS SAWR sensors tested at OSU-NRL remained functional during testing. In addition, once the sensor radioactivity levels were deemed safe for transport and handling i.e., < 1 µC, all seven SAWR devices were returned to UMaine facilities for post-irradiation analysis. Measurements of the sensors showed no signs of degradation with respect to their pre-irradiation resonant frequencies and signal strengths.

Regarding the exposure to radiation, the tests at OSU-NRL revealed that, in general, the Pt-Al_2O_3 electrode sensors were more sensitive to detecting neutron flux than the devices with Pt-Ni electrodes. In addition, measurements conducted at room temperature showed that significant

Continued on next page

Continued from previous page

gamma heating of the LGS SAWR devices occurred over the range of reactor powers tested (e.g., up to 90°C at 300 kW), and in general must be accounted for when measuring SAWR frequency shifts that are only due to neutron flux induced material softening.

Fig. 26a shows a representative sensor frequency response overlaid with the reactor power levels used to irradiate the sensor probes at 800°C. Use of the furnace temperature controller ensured a constant sensor temperature during these measurements, meaning the frequency variations shown in Fig. 26a were primarily due to variations in neutron flux and not significantly influenced by variations in gamma heating. As shown in Fig. 26a, the sensor frequency response shifts to lower frequencies when exposed to different reactor powers, which is consistent with a softening in the elastic constants of the SAWR electrodes.

Fig. 26a also shows that larger shifts in reactor power corresponded to larger frequency shifts. Specifically, the LGS SAWR sensors produced linear frequency shifts at an approximate rate of -3 kHz / 100 kW. As such, this approach shows the feasibility of using LGS SAWR technology for monitoring in-core neutron flux rates at temperatures up to 800°C.

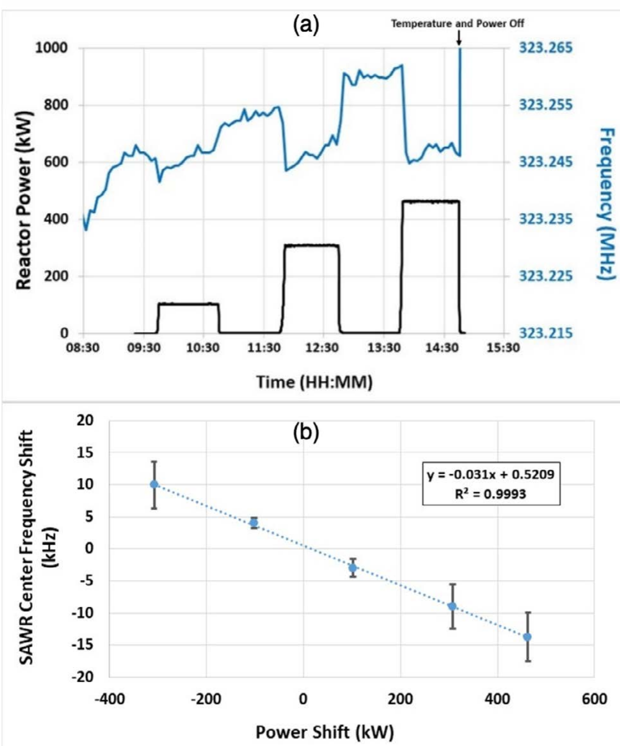

Fig. 26. (a) Representative LGS SAWR sensor with Pt-Al2O3 electrodes showing frequency response at 800°C versus different reactor power levels. (b) Average frequency shift versus reactor power shift. Reproduced from reference 3.

Conclusion and Future Work

The proof-of-principle work described here is an important step towards the development of much needed sensor technologies capable of providing monitoring and prognostic capabilities in harsh environments present within advanced high temperature nuclear reactors. Future work will focus on continued testing of the LGS SAWR sensor platform at higher reactor powers and over longer test periods for technology maturation, and for use in various advanced reactor applications.

Acknowledgements

This work is supported by the Nuclear Regulatory Commission (NRC) under Award Number 31310023M0009, and by the U.S. Department of Energy, Office of Nuclear Energy under DOE Idaho Operations Office Contract DE-AC07- 051D14517 as part of a Nuclear Science User Facilities program experiment.

References

[1] N. C. Anheier, "Technical readiness and gaps analysis of commercial optical materials and measurement systems for advanced small modular reactors", Pacific Northwest National Laboratory (PNNL), Richland, WA, USA, No. PNNL-22622 Rev. 1, Aug. 2013.

[2] K. Korsah, "Assessment of Sensor Technologies for Advanced Reactors", Oak Ridge National Laboratory (ORNL), Oak Ridge, TN, USA, No. ORNL/TM-2016/337, Aug. 2016.

[3] L. D. Doucette, M. G. Greenslit and M. Pereira da Cunha, "Nuclear Irradiation and Characterization of Langasite SAWR Sensors up to 800 °C," in IEEE Transactions on Ultrasonics, Ferroelectrics, and Frequency Control, vol. 72, no. 2, pp. 169-177, Feb. 2025.

[4] G. Sha, C. Harlow, A. Chernatynskiy, J. Daw, and M. Khafizov, "In-situ measurement of irradiation behavior in $LiNbO_3$", Nuclear. Instruments and. Methods Phys. Res., B, vol. 472, pp. 46-52, 2020.

[5] Y. Wang, G. Sha, C. Harlow, M. Yazbeck, & M. Khafizov, "Impact of nuclear reactor radiation on the performance of AlN/sapphire surface acoustic wave devices", Nuclear Instruments and Methods Phys. Res., B, vol. 481, 35-41, 2020.

[6] A. Maskay, A. Ayes, R. J. Lad, & M. Pereira da Cunha, "Stability of Pt/Al2O3-based electrode langasite SAW sensors with Al2O3 capping layer and yttria-stabilized zirconia sensing layer", IEEE International Ultrasonics Symposium pp. 1-4, Sept. 2017.

[7] M. Pereira da Cunha, A. Maskay, R. J. Lad, D. J. Frankel, S. Moulzolf, M. Call, and G. Bernhardt, "Pt-Ni/Pt-Zr electrodes for stable SAW resonator operation during repeated temperature cycling up to 1000° C", IEEE International Ultrasonics Symposium (IUS), pp. 1-4, Oct. 2015.

[8] M. Pereira da Cunha, "High-temperature harsh-environment SAW sensor technology", 2023 IEEE International Ultrasonics Symposium., pp. 1-10, September 2023.

Johnson Noise Thermometry for In Situ Recalibration of RTDs in Nuclear Reactors

Daniel C. Sweeney
Oak Ridge National Laboratory

F. Kyle Reed
Oak Ridge National Laboratory

N. Dianne Bull Ezell
Oak Ridge National Laboratory

Abstract

Resistive temperature devices (RTDs) are used in the nuclear industry to measure critical temperatures, such as the temperature differential across a reactor's core and its thermal output. Though RTDs reduce drift, relative to thermocouples, irradiation damage accumulation from the high neutron and gamma radiation environments in and around reactors nonetheless results in measurement drift, particularly over long periods of exposure. This drift increases measurement uncertainty and increases the periodic maintenance requirements for RTDs deployed in high radiation environments. Previously, Johnson noise thermometry (JNT) has been used to mitigate drift artifacts in RTD-based temperature measurements in high-energy physics application through measurements of thermal noise amplitude, which are proportional to absolute temperature. To demonstrate the feasibility of using JNT for in situ recalibration RTDs exposed to neutron and gamma radiation, a JNT instrument is under development at Oak Ridge National Laboratory. This instrument is designed around a commercially available combined analog front-end and analog-to-digital converter designed to perform four-wire measurements designed and characterized for operation in space radiation conditions. Nuclear radiation-tolerant circuitry enabling recalibration of RTDs in situ would drive down maintenance costs and improve the reliability of RTD measurements and their lifetimes in nuclear environments.

Introduction

Accurate temperature measurements are critical to the safe and effective production of nuclear energy. For example, temperature measurements across the reactor core are used in the measurement of thermal power output of a reactor. Additionally, safety-critical temperature measurements provide online data to ensure that components are maintained within their safe thermal limits. RTDs and thermocouples are installed throughout a reactor and the surrounding facility to acquire these measurements. RTDs are typically fabricated from platinum (Pt) with a DC resistance of 100 Ω (Pt-100) or 1000 Ω (Pt-1000) measured at 0°C and exhibit a lower uncertainty, higher reliability, and less radiation-induced drift than thermocouples [1-3]. RTDs often require complex front-end circuitry to achieve the desired measurement accuracy and precision. Despite these benefits, RTDs suffer from calibration drift in resulting from insulation degradation, corrosion, and radiation damage (transmutation, lattice damage, gamma heating, etc.) in both the sensing element and lead wires [4,5]. To compensate for changes in lead wire impedance, additional leads can be added. For example, the simplest method to measuring the resistance of an RTD is a 2-wire measurement, in which the voltage across a resistor bridge containing the RTD is compared with a reference voltage (Fig. 27a). 3- and 4-wire measurements add leads to one or both sides of the RTD and enable the impedance changes of the leads to be mitigated. Though these leads could be added to a similar bridge circuit, as used with a 2-wire RTD measurement, the current injected into the RTD is monitored and a differential amplifier is used to measure the voltage difference across it. In this way, the high-impedance inputs to the amplifier do not allow significant current to flow through their RTD-connected leads and enable a precise measurement of the RTD and the effects of the lead cables mitigated.

Despite the high precision and reliability achievable with RTDs, long-term exposure to nuclear reactor environments nonetheless results in measurement drift arising from transmutations, lattice defects, gamma heating, and other effects [5]. To enable reliable measurements of RTDs to be performed, they must be frequently re-calibrated. Conventional re-calibration techniques involve making measurements with a known reference and are challenging to perform, particularly in smaller, next-generation reactor concepts. For example, terrestrial small modular reactors (SMRs) and space reactors are both intended for 3 to 5 years of continuous operation and autonomous operation without significant manual intervention. Performing RTD recalibrations while in space or when reactors are deployed in resource-limited environments imposes a significant technical and regulatory hurdle. To overcome this challenge, a method to enabling RTDs to be recalibrated in situ using thermal electron (Johnson) noise, commonly used in high energy physics, is being adapted for the high temperature, neutron/gamma mixed radiation reactor environments. This JNT system utilizes an existing commercial-off-the-shelf (COTS) integrated

Continued on next page

Continued from previous page

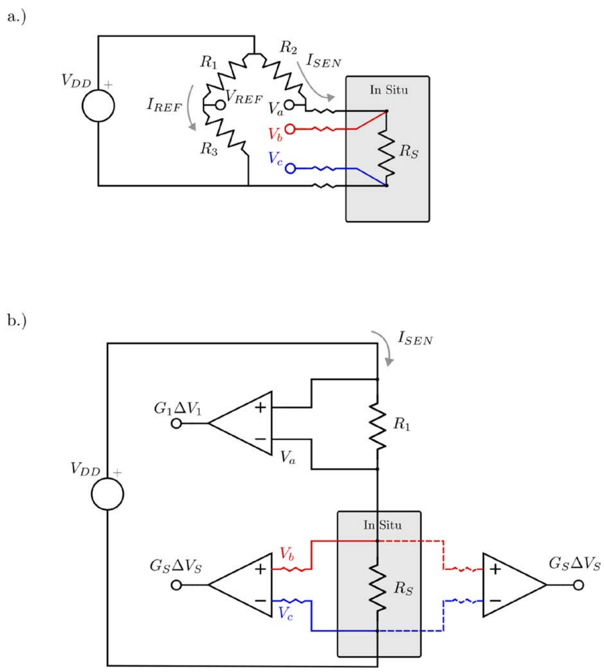

Figure 27. Resistance temperature devices (RTDs) can be performed in 2-, 3-, and 4-wire configurations using a bridge circuit (a.) or active components (b.)

circuit designed for performing 4-wire measurements. This front-end circuitry has been demonstrated to survive space radiation environments and has an integrated analog-to-digital converter (ADC), which facilitates integration with read-out circuitry. This system will be tested in a research reactor to both demonstrate JNT measurements in reactor environments and the performance of space-characterized 4-wire COTS circuitry within a terrestrial nuclear environment. This design and the irradiation data will provide insight into the feasibility of utilizing JNT for in situ recalibration of RTDs installed in reactors and a means to potentially drive down the associated maintenance costs.

Signal Processing and Analysis

The thermal electron noise (Johnson noise) in an RTD is proportional to the bandwidth measurement, the resistance of the Pt-100 or Pt-1000 element, and the absolute temperature of the RTD (<1 GHz) [4]. Using a differential voltage measurement across a shunt resistor to measure the current injected into the RTD, the impedance of the RTD can be measured using a second differential voltage measurement (Fig. 27b). This measurement is the sum of the Johnson noise, noise introduced by the amplifier, and the resistance of the RTD. To measure the Johnson noise, a second amplifier is introduced to perform the same differential voltage measurement across the RTD. The cross-power spectral density (CPSD) of these two amplified measurements allows the Johnson noise to be isolated from the uncorrelated amplifier noise. High-order, low-pass filters are also introduced to eliminate the DC component of the RTD measurement, corresponding to the DC resistance of the RTD, which isolates the Johnson noise.

To perform these measurements, custom circuit boards were designed to facilitate connections between the RTD, the 4-wire ADC intended for irradiation environments, and leads for digital communication and additional measurements intended to be performed during testing. A microcontroller-based data acquisition and storage platform facilitates data transfer between the 4-wire ADC and a host computer where data will be logged and the CSPD-based digital signal processing will be performed. As part of this effort, performance of Pt-100 and Pt-1000 RTDs will both be characterized prior to irradiation testing to identify the configuration likely to provide the highest signal integrity.

Conclusion

Enabling online re-calibration of RTDs during reactor operation will mitigate maintenance costs and lengthen the reactor up-time. Here, we intend to demonstrate the feasibility of using JNT to re-calibrate RTDs online in nuclear reactors. The technologies and techniques developed in this work provide precedent for utilizing electrical components intended and characterized for space radiation environments to improve the performance of terrestrial reactor instrumentation.

References

[1] Leonard, J. H., & Hunkar, D. B. (1967). Direct radiation effects on thermocouples. Nuclear Applications, 3(12), 718-727.

[2] Qian, T, Hinds, H W, & Tonner, P. (1997). Self-heating, gamma heating and heat loss effects on resistance temperature detector (RTD) accuracy. Canada. INIS-CA-0071.

[3] Hashemian, H. M., & Jiang, J. (2009). Nuclear plant temperature instrumentation. Nuclear Engineering and Design, 239(12), 3132-3141.

[4] Kisner, R., Britton, C. L., Jagadish, U., Wilgen, J. B., Roberts, M., Blalock, T. V., ... & Ericson, M. N. (2004). Johnson noise thermometry for harsh environments. 2004 IEEE Aerospace Conference Proceedings. Big Sky, MT, USA, Vol. 4 pp. 2586-2596 Vol.4

[5] Ross, C. W. (1961). Effect of Thermal Neutron Irradiation on Thermocouples and Resistance Thermometers. IRE Transactions on Nuclear Science, 8(4), 110-118.